THE JOURNAL OF PHYSICAL CHEMISTRY A

Article

Cite This: J. Phys. Chem. A 2019, 123, 9123−9131

pubs.acs.org/JPCA

Room-Temperature Phosphorescence from Encapsulated Pyrene Induced by Xenon

A. Mohan Raj, Gaurav Sharma, Rajeev Prabhakar,* and V. Ramamurthy*

Department of Chemistry, University of Miami, Coral Gables, Florida 33146, United States

Supporting Information

ABSTRACT: Phosphorescence from pyrene especially at room temperature is uncommon. This emission was recorded utilizing a supramolecular organic host and the effect due to the heavy atom. Poor intersystem crossing from S_1 to T_1, small radiative rate constant from T_1, and large rate constant for oxygen quenching hinder the phosphorescence of aromatic molecules at room temperature in solution. In this study, these limitations are overcome by encapsulating a pyrene molecule within a water-soluble capsule (octa acid, OA) and purging with xenon. While OA suppressed oxygen quenching, xenon enabled the intersystem crossing from S_1 to T_1 and radiative process from T_1 to S_0 through the well-known heavy atom effect. The close interaction facilitated between the pyrene and the heavy atom perturber xenon in the three-component supramolecular assembly (OA, pyrene, and xenon) resulted in phosphorescence from pyrene. Computational modeling and NMR studies supported the postulate that pyrene and more than one molecule of xenon are present within a confined space of the OA capsule.

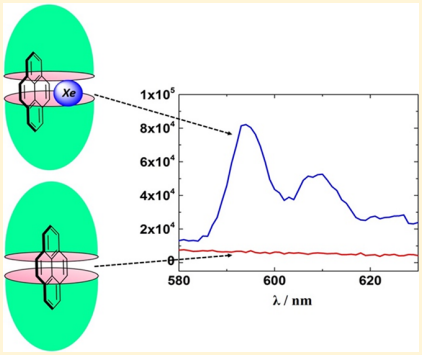

INTRODUCTION

Recent upsurge[1−6] in "up-conversion", a process prompted by triplet−triplet annihilation,[7] has led to exploring new methods in enhancing the generation of molecules in their triplet states (T_1) at room temperature in solution.[8−16] Though the theory of the "heavy atom effect", one of the well-known methods to enhance triplet yields of aromatics in solution due to Kasha and his co-workers is well understood,[17−20] and its usefulness in inducing phosphorescence in isotropic solution is limited due to quenching of the triplets by dissolved oxygen. However, the value of the heavy atom effect has been established in supramolecular assemblies (micelles, cyclodextrins, zeolites, and silica),[21−35] which by confining the aromatic guest molecules and protecting their excited state from the quencher oxygen[36,37] also bring the heavy atom (or ion) closer to elicit room temperature phosphorescence of the guest aromatic molecule. Unlike Tl^+, the heavy atom valued for bringing about phosphorescence at room temperature from supramolecular encapsulated guests including in the recent example with an organic cavitand and pyrene as the host and guest, respectively,[8] and heavy atom xenon, soluble in isotropic solvents,[38] has attracted little attention.[39] Although xenon's effect on intersystem crossing (S_1 to T_1 and T_1 to S_0) is well documented,[40−46] very few publications mention about xenon-induced phosphorescence in solution at room temperature. The continued interest[8] on room-temperature phosphorescence[47] employing supramolecular assemblies motivated us to examine the process using octa acid (OA, Figure 1b)[48,49] as the host and xenon and Tl^+ as the heavy atom perturbers. In addition, our interest in energy, electron, and spin transfer across the OA capsular wall[49,59] prompted us to explore the possibility of singlet−triplet spin perturbation by heavy atoms under similar circumstances.[50−58]

Recently, we demonstrated that the phosphorescence from thioketones at room temperature in solution could be enhanced by confining them within an octa acid capsule.[60] Such confinement suppressed the prevalent self-quenching of the excited thioketone by a ground state thioketone of the same kind, which is a major cause for lack of phosphorescence from thioketones.[61] Given that aromatic molecules have poor S_1 to T_1 intersystem crossing and T_1 to S_0 radiative rate constants and the triplets are quenched by oxygen at the diffusion-controlled rate, we wished to explore the value of the OA capsule in bringing out the phosphorescence from these molecules.[62] We envisioned that the OA capsular assembly would keep the quencher oxygen away and heavy atoms such as xenon and Tl^+ present in solution would enhance the rates of S_1 to T_1 intersystem crossing and T_1 to S_0 radiative processes. In this report, the results of our study focused on enhancing phosphorescence from pyrene, a model for aromatic molecules, in aqueous solution by employing supramolecular and heavy atom strategies are discussed. We chose pyrene because it can be solubilized in a buffer solution by the cavitand OA.[63,64] Also such a host−guest assembly does not phosphoresce in aqueous solution at room temperature even when it is saturated with nitrogen. To our surprise, when the solution of py@OA_2 (1:2 capsule) was saturated with xenon, phosphorescence from pyrene was observed. On the other

Received: September 2, 2019
Revised: September 18, 2019
Published: September 22, 2019

Downloaded via UNIV OF MIAMI on July 17, 2020 at 15:46:31 (UTC).
See https://pubs.acs.org/sharingguidelines for options on how to legitimately share published articles.

© 2019 American Chemical Society

DOI: 10.1021/acs.jpca.9b08354
J. Phys. Chem. A 2019, 123, 9123−9131

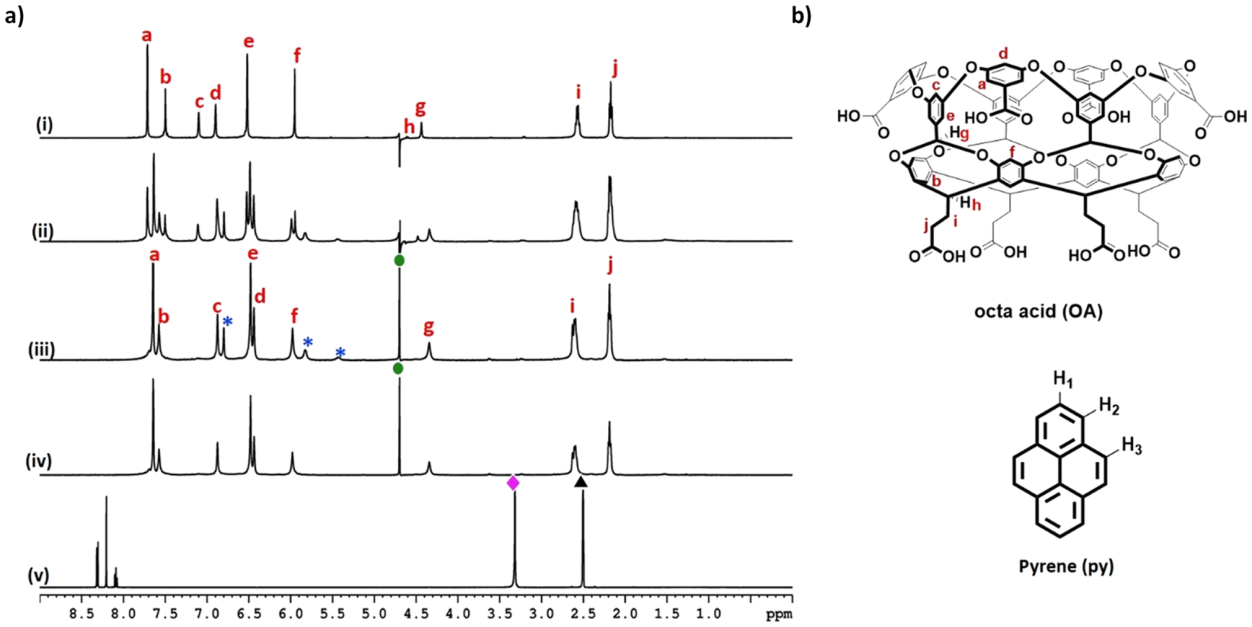

Figure 1. (a) ^{1}H NMR (500 MHz) spectra of (i) OA(1 mM) in 10 mM $Na_2B_4O_7$ buffer/D_2O, (ii) py@OA ([OA] = 1 mM), [py] = 0.25 mM), (iii) py@OA ([OA] = 1 mM), [py] = 0.5 mM), (iv) py-d_{10}@OA ([OA] = 1 mM), [py-d_{10}] = 0.5 mM), and (v) py in DMSO-*d*6. "*" indicates the bound guest proton peak, and "green circle solid", "pink diamond solid", "black triangle up solid" represent the residual water, HOD, and DMSO, respectively. (b) Chemical structure of host (OA) and guest (py).

hand, the heavy cation Tl^+ that is established to induce phosphorescence from aromatics included in micelles, zeolites, and cavitands failed to induce phosphorescence from OA-encapsulated pyrene. The results with these heavy atoms (ion) perturbers discussed below bring out the distinct value (and limitation) of the heavy atom technique with the aromatic@OA_2 supramolecular assembly.

EXPERIMENTAL SECTION

Materials and Methods. The host octa acid was synthesized following the published procedure. Pyrene was recrystallized with ethanol and used in the study. Deuterated pyrene was purchased from MSD Isotopes. ^{1}H NMR spectra were recorded at room temperature under aerated conditions on a Bruker 500 MHz NMR. Steady-state fluorescence spectra were recorded using an Edinburgh FS920CDT fluorimeter and time-resolved measurements were carried out on an Edinburgh FL900CDT spectrometer.

General Procedure for Guest Binding Studies Probed by NMR. A D_2O stock solution (600 μL) of the host OA (1 mM) and sodium borate buffer (10 mM) taken in an NMR tube was titrated with the guest by sequential addition of 0.25 equiv of guest (2.5 μL of a 60 mM solution in DMSO-d_6). The complexation was achieved by sonicating the NMR tube for about 5 min. The 1:2 complex was achieved with 5 μL of the guest solution to 600 μL of OA. ^{1}H NMR spectra were recorded after purging with Xe gas for 10 min.

^{129}Xe NMR Experiments. ^{129}Xe NMR experiments were performed on a Bruker Avance III-HD 400 MHz spectrometer (110.73 MHz) using a 5 mm Prodigy (liquid Nitrogen based) board band Cryoprobe. The spectra were collected using a 500 ppm spectral width, centered at −5275 ppm. Chemical shifts were reported with respect to $XeOF_4$ and calculated by Topshim 3.6.1 from the deuterium lock frequency and no further reference. FID acquisition times of 0.5 s were collected with either 6 or 20s relaxation delay and the sample temperature was regulated at 25 °C. The samples were prepared by first sonicating for 20 min the solution of the Py@OA complex prepared as mentioned above prior to 5 min bubbling with Xe gas (Matheson Gas, 99.999%) and pressurized to 2 atm of Xe and the tubes were sealed (J-Young valves).

Fluorescence and Phosphorescence Measurements. A stock solution of 5 μM pyrene was prepared by adding 5 μL of solution (2 mM pyrene in methanol) to 2 mL of borate buffer solution. To the solution, OA was slowly added (0−25 μM) from a stock solution of 1 mM in borate buffer and corresponding spectra were recorded. The py@OA_2 complex was purged with Xe gas for 10 min and the emission spectra were recorded for room-temperature phosphorescence. Similarly, thallium nitrate (100 mM stock solution) was also gradually added to the py@OA_2 complex and corresponding emission spectra were recorded.

Computational Procedure. The three-dimensional structure of OA was obtained from our previous work[65] and pyrene was modeled using the GaussView program. Both OA and pyrene were optimized without any geometrical constraint at the B3LYP[66]/6-31g(d)[67] level using the Gaussian 09 program.[68] They were parameterized using the generalized Amber force field (GAFF) utilizing the antechamber program, an inbuilt tool in the AMBER software package.[69] The parameters for xenon were obtained from a previous work by Goharshadi and Abbaspour.[70] To obtain the initial binding poses of pyrene inside the OA capsule, molecular docking was performed using the Autodock Vina1.5.6 software.[71] In this procedure, the size of the grid was chosen to cover the entire OA and the spacing was kept to 1.00 Å, a standard value for Autodock Vina. The molecular dynamics (MD) simulations of OA with a guest molecule were performed using the GROMACS4.5.6[72] program. The starting structures were placed in a cubic box with dimensions of 60 × 60 × 60 Å

DOI: 10.1021/acs.jpca.9b08354
J. Phys. Chem. A 2019, 123, 9123−9131

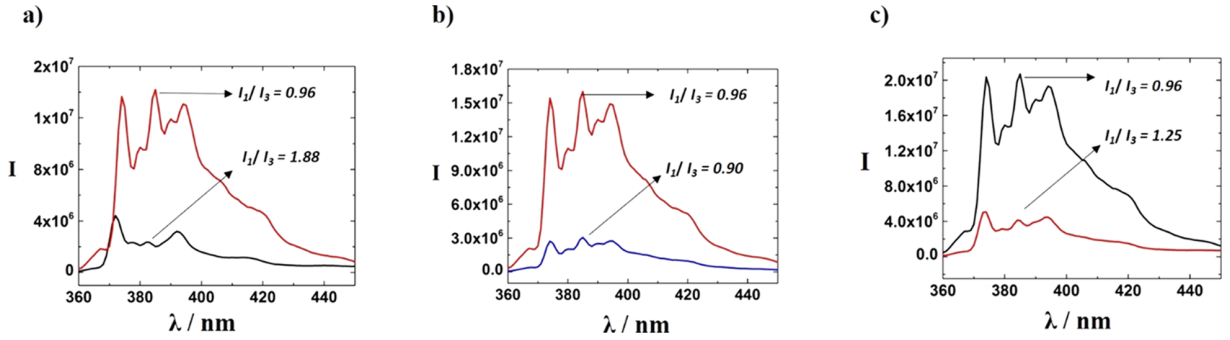

Figure 2. Changes in I_1/I_3 value. (a) Emission spectra of py in borate buffer (black) after OA added (red); (b) Emission spectra of py@OA_2 complex before Xe purged (red) and after Xe purged (blue); (c) Emission spectra of py@OA_2 complex before thallium addition (black) and after thallium added (red).

and filled with explicit TIP3P water molecules.[73] The shortest distance from the surface of the OA to the edge of the box was 1.0 nm. Electrostatic interactions were calculated using the particle mesh Ewald method,[74] and a cutoff at 1.2 nm was used for both van der Waals and Coulombic interactions. Charge neutrality was maintained by adding an appropriate number of sodium ions. The OA−guest complexes were energy minimized for 3000 steps by the steepest descent method, which resulted in the formation of the starting structure for MD simulations. The simulations were carried out with a constant number of particles (N), pressure (P), and temperature (T) (NPT ensemble). The SETTLE[75] algorithm was used to constrain the bond length and angle of the water molecules, and LINCS[76] algorithm was employed to constrain the bond lengths of the OA and guest molecule. For all the systems, a 100 ns production run was performed. The MD trajectories were computed for each model with a time step of 2 fs. To obtain the most representative structures of the OA−guest complex, a cluster analysis was performed. Finally, Yasara,[77] VMD,[78] and Chimera[79] programs were used for the analysis of the MD trajectories and preparation of figures.

RESULTS AND DISCUSSION

OA is established to form a closed capsule with aromatic molecules as guests.[64,80] As expected, OA encapsulates one molecule of pyrene to form a 1:2 capsule. ^{1}H NMR spectra of pure OA, pyrene, and the pyrene@OA_2 presented in Figure 1a and Figures S1 and S2 (Supporting Information) confirm the inclusion of pyrene within OA. The several new signals due to OA (Figure 1a-ii) that appear upon initial addition of pyrene to a borate buffer solution of OA are assigned to free and complexed OA. Further addition of pyrene (1 equiv of pyrene to 2 equiv of OA) resulted in the disappearance of signals due to free OA. The fact that no free signals due to OA were seen following the addition of half an equivalent of pyrene suggested that it formed a 1:2 capsule with OA. The measured diffusion constant for the pyrene−OA complex of 1.4×10^{-6} cm^2/s by DOSY experiments (Table S1)[80] relative the free OA's of 1.8×10^{-6} cm^2/s confirms the complex to be a 1:2 capsule. Signals due to pyrene (starred peaks in Figure 1a-iii) were assigned based on the COSY spectrum (Figure S3). Further, the use of perdeuterated pyrene as the guest confirmed the assignments. In spectrum of Figure 1a-iv, as expected no signals due to the guest were seen when perdeuterated pyrene was the guest, although that due to the OA capsule had the same chemical shifts as in the case of the pyrene−OA complex. We believe the pyrene molecule to be located in the middle region of the capsule (Figure S4b), which is confirmed by NOESY spectra (Figure S4a), where the H_3 hydrogens of pyrene and H_d hydrogens of OA appear to be near. The structure of this complex derived from molecular dynamics (MD) simulations is consistent with this inference (Figure S4c). In this structure, pyrene interacts with the walls of OA through both CH−π (~2.8 Å) and $\pi-\pi$ interactions (~3.5 Å).

Knowledge of the effect of heavy atoms on the stability of the pyrene@OA_2 capsule was necessary in going forward with our study on the influence of these atoms on the emission of the encapsulated guest. The capsule has been established to partially open and close in a timescale of 5 μs and fully disassemble and assemble in 2.7 s and the assembly's interior to be nonpolar (closer to benzene) with the help of fluorescent probes.[63,81−83] Consistent with the intensities of 1 and 3 vibrational bands (I_1/I_3 ratio) of pyrene's fluorescence spectra being indicators of the surrounding polarity, the value within the OA capsule has been reported to be 1.01, closer to that in benzene.[84−86] We speculated the I_1/I_3 ratio of ~1.0 of OA-encapsulated pyrene to increase on exiting it or on exposure to the aqueous exterior environment. With this in mind, the fluorescence of the pyrene@OA_2 complex in the presence of heavy atom perturbers $TlNO_3$ and xenon was recorded. The emission spectra of pyrene in borate buffer, in the presence of OA (Figure 2a) and pyrene@OA_2 in the presence and absence of Xe and $TlNO_3$, are presented in Figure 2b,c, respectively. Expectedly, the I_1/I_3 decreases from 1.88 in the buffer solution to 0.96 upon addition of OA (Figure 2a and Figure S5), shifting closer to that in benzene. This confirmed that the pyrene is encapsulated within OA with a benzene-like environment. The slight decrease in I_1/I_3 from 0.96 to 0.90 on bubbling xenon into the solution suggested the surroundings of pyrene going even less polar than benzene. Although this might be due to xenon co-occupying the capsule with pyrene, it unequivocally indicated that xenon does not displace pyrene from the OA capsule. On the other hand, Figure 2c suggests that the pyrene experiences a more polar environment (the I_1/I_3 changes from 0.96 to 1.25) upon addition of $TlNO_3$. The ^{1}H NMR and fluorescence spectra at various added concentrations of $TlNO_3$ are provided in Figure S6. Addition of $TlNO_3$ resulting in appearance of weak excimer emission (Figure S6b inset) and a steady increase in the I_1/I_3 ratio (Figure S7) indicate increased exposure of pyrene to water molecules. These observations lead us to propose that upon addition of $TlNO_3$, the capsule opens up slowly to expose the guest (pyrene) to the aqueous medium. The excimer formation

DOI: 10.1021/acs.jpca.9b08354
J. Phys. Chem. A 2019, 123, 9123−9131

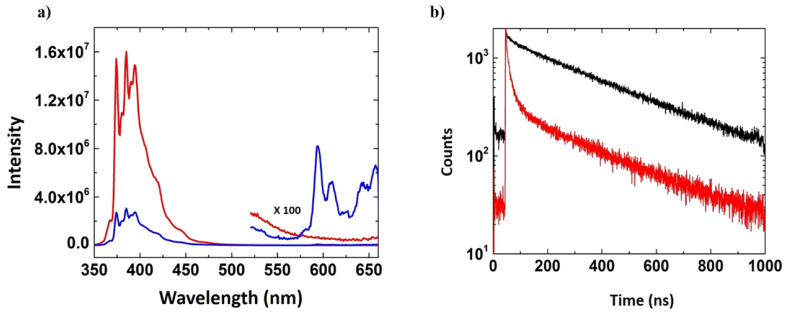

Figure 3. (a) Emission spectra of py@OA_2 complex (red) and py@OA_2 + Xe purged for 10 min (blue) (λ_{exc} = 337 nm); Phosphorescence spectra around 580 to 650 nm of py@OA_2 observed (blue) after Xe purging were scaled up by 100 and shown in the figure. (py = [5 μM], OA = [25 μM]); (b) Time-resolved fluorescence decay of py@OA_2 complex (black) and py@OA_2 + Xe purged for 10 min (red).

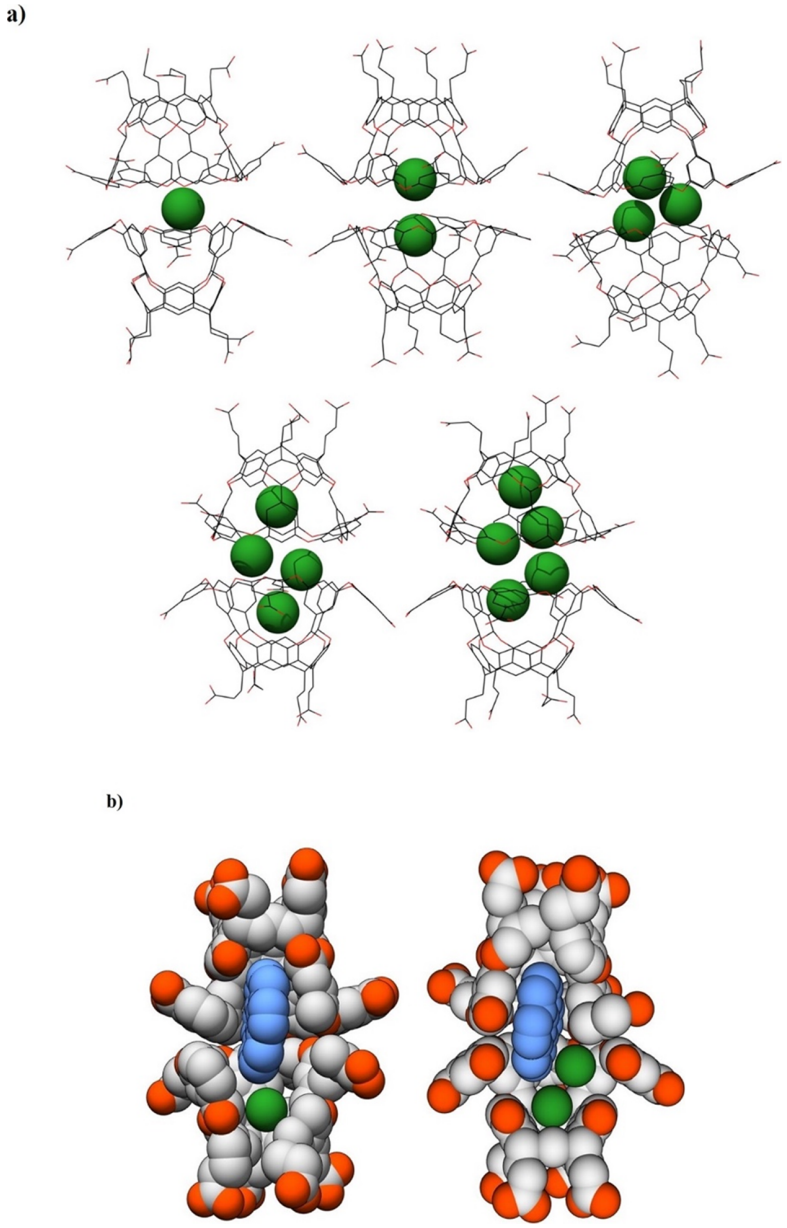

Figure 4. (a) MD simulated possible structures of encapsulation of Xe with OA; (b) The most representative structures of OA encapsulating pyrene + one Xe atom and two Xe atoms obtained from MD simulations.

DOI: 10.1021/acs.jpca.9b08354
J. Phys. Chem. A 2019, 123, 9123−9131

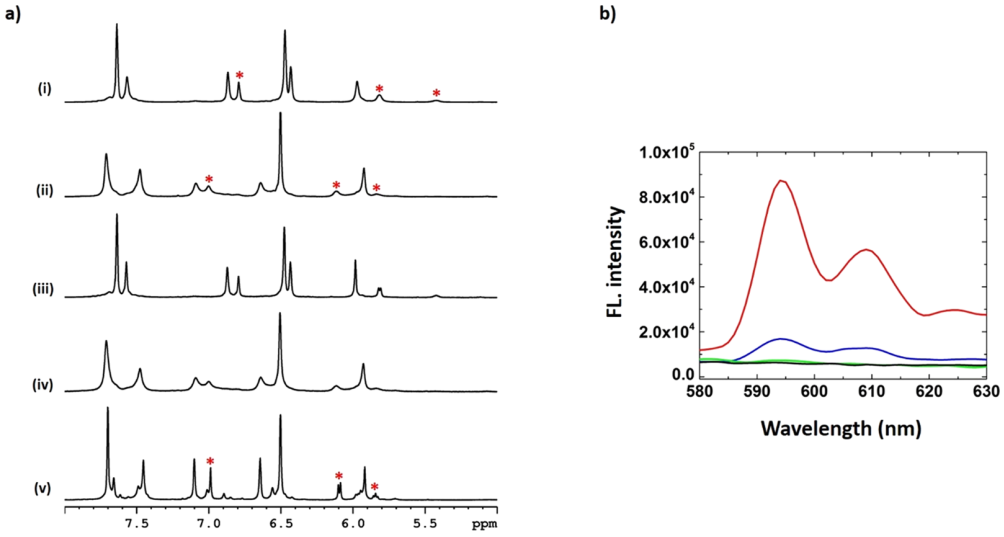

Figure 5. (a) Partial ^{1}H NMR (500 MHz) spectra of py@OA_2: (i) aerated, (ii) after Xe purged, (iii) after N_2 purged, (iv) after Xe purged, and (v) Py@OA_2 + Xe purged at 2 °C; "*" represents the bound pyrene protons. (b) Phosphorescence spectra of py@OA_2: aerated (black), after N_2 purged (blue), after Xe purged (red), and after O_2 purged (green).

suggests escaping of some molecules from the capsule and aggregating in water. These results hinting that the capsule is not stable in the presence of $TlNO_3$ and is not surprising based on earlier results in the presence of excess NaCl.[80] Consistent with this conclusion, the ^{1}H NMR signals become broader with increased addition of $TlNO_3$ (Figure S6a compare (i) and (vi)). Thus, while the capsule is stable in the presence of heavy atom xenon, it is not stable in the presence of heavy cation Tl^+ and no phosphorescence was observed in its presence as can be seen in Figure S6b. We therefore focused our further studies related to heavy atom-induced phosphorescence with Xe as the perturber.

The emission spectrum of pyrene@OA_2 in borate buffer under aerated and Xe-saturated conditions is presented in Figure 3. These spectra bring out two important points: (a) The capsule remains closed during the excited S_1 lifetime of pyrene; the I_1/I_3 ratio is unaffected by the presence of xenon. (b) Importantly, pyrene exhibiting no phosphorescence in aerated buffer solution does phosphoresce in Xe-saturated solution (>575 nm). Comparison of the spectra in Xe-saturated buffer (without OA) and cyclohexane (Figure S8) with that of pyrene@OA_2 in buffer (Figure 3a) suggests that Xe is effective as the heavy atom perturber inducing phosphorescence only when pyrene is within the OA capsule. Besides, this study such an effect of Xe on phosphorescence is only known in zeolites at 77 K and none in solution.[39] Xe's impact on S_1 to T_1 intersystem crossing in aromatics and enones has been documented.[40−42,44,46] This phosphorescence is observed only from pyrene@OA_2 suggested that the perturber Xe and the emitter pyrene must be close to each other. Xe being ineffective in solution but effective in bringing about phosphorescence in solid zeolites indicated the need for the emitter and Xe to be close proximity for a longer time. OA seems to bring the two molecules closer and keep them together for the time required for spin−orbit perturbation to operate. Computational modeling and Xe NMR experiments were conducted to probe the location of Xe in a buffer solution containing the host OA.

Feasibility of inclusion of Xe within a number of hosts dissolved either in organic solvents or in water has been confirmed through Xe NMR experiments.[87−91] The internal volume of the empty OA capsule was estimated to be 1002 Å^3 by first filling it with dummy beads and then calculating their total volume using the YASARA program.[77] Since the volume of the Xe atom is 42 Å^3, we expected several Xe atoms would be included within the OA capsule. Sequential addition of Xe atoms with the help of the data from modeling of Xe−OA interactions by placing a Xe atom inside the OA capsule (Figure 4a) showed that the OA capsule can occupy up to five Xe atoms. The addition of the sixth Xe atom led to one of these atoms to exit the capsule that opened up. In all these complexes, Xe atoms weakly interacted by maintaining a distance of 4.0−5.5 Å with each other and 3−4 Å with the walls of OA. It is noteworthy that these MD simulations did not reveal the most stable structure. We did not pursue the complexation of OA with Xe further as it was beyond our goal of the effect of Xe on pyrene's emission. To obtain experimental evidence for the inclusion of Xe within the OA capsule, Xe NMR spectra of the buffer solutions with and without Xe were recorded (Figure S9). We interpret the sharp signal in the absence of OA in D_2O that shifted downfield and broadened in its presence to be indicative of multiple xenon atoms occupying the OA capsule. Further experiments are required to confirm the conclusion.

To gain an understanding of the mechanism of xenon's effect on the emission of encapsulated pyrene, it is important to know its location in the presence of OA and pyrene. In principle, Xe could be either in water, not adjacent to pyrene, or within the OA capsule along with pyrene. Once again, we resorted to computational modeling to probe whether there is enough space for both Xe and pyrene within the OA capsule. MD simulations suggested that one or two Xe atoms can co-occupy a capsule with pyrene (Figure 4b). In the Xe_1.py@OA_2 complex, the Xe atom was located 3.0 Å away from pyrene. As shown in Figure S9 and Figure 4a, it is along the long axis of the capsule with the OA−py and OA−Xe distances being 3.0 and 2.9 Å, respectively. This weak Xe−py interaction can polarize the py molecule. On the other hand, in the Xe_2.py@OA_2 complex, the second Xe atom occupies the equatorial position with respect to the pyrene ring (3.7 Å). Such an

DOI: 10.1021/acs.jpca.9b08354
J. Phys. Chem. A 2019, 123, 9123−9131

orientation results in weaker interaction between pyrene and the two Xe atoms (3.4 and 3.7 Å; Figure S9). The crowding of the capsule in the presence of the two Xe atoms pushes the pyrene closer to the walls of OA, that is, 2.5 Å. A comparison of the complexation energy of these molecules shows that Xe_2.py@OA_2 is 34.0 kcal/mol more stable than the Xe.py@OA_2 complex. This energy was calculated by subtracting the energies of the bound complexes and their unbound constituents, that is, $\Delta E_1 = E_{Xe.py@OA2} - (E_{OA2} + E_{Xe} + E_{py})$ and $\Delta E_2 = E_{Xe2.py@OA2} - (E_{Xe.py@OA2} + E_{Xe})$. Based on IR spectroscopic measurements and quantum chemical calculations, the existence of weak interactions between xenon and aromatic molecules such as toluene and *p*-cresol has been speculated.[92] Thus, the possibility of weak interaction between pyrene and Xe is not unprecedented. Such types of weak interactions between the capsular wall that is predominantly aromatic and Xe would favor Xe to reside within the OA capsule rather than in water. A clue to the Xe residing within the OA capsule along with pyrene came from the Xe NMR spectrum (Figure S10). The Xe NMR signal was significantly different from that of Xe in water in the absence and presence of OA. While the signal was broad in OA, it was sharper in the buffer solution containing py@OA_2. At the same time, it was downfield shifted to that in pure water. We tentatively ascribe this to Xe being present within OA along with pyrene.

Additional support for the above conclusion came from ^{1}H NMR spectra of py@OA_2 in the presence of air, Xe, and nitrogen (Figure 5). Signals due to OA that were relatively sharp in an aerated medium (Figure 5i) became broader when solution was saturated with Xe (Figure 5ii). When the same solution was bubbled with nitrogen, the signals became sharper (Figure 5iii). In this case, the xenon was displaced with nitrogen and the solution must contain only the py@OA_2 complex and nitrogen. Finally, when this solution was bubbled with Xe again, the signals became broader similar to Figure 5ii. This change in spectra with alternate Xe and N_2 bubbling reveals that the two gases are weakly held within the capsule and could be easily exchanged. From these experiments, we conclude that the ^{1}H NMR spectrum is broader in the presence of xenon. No changes in the positions of OA ^{1}H NMR signals suggest that although Xe can be displaced, the encapsulated pyrene cannot be easily displaced through bubbling with either xenon or nitrogen.

One could visualize the presence of at least four types of complexes when buffer solution of py@OA_2 is saturated with Xe: py@OA_2, Xe@OA_2, Xe_1.py@OA_2, and Xe_2.py@OA_2. Molecular modeling as illustrated in Figure 4b suggests that one or two molecules of Xe can co-occupy a capsule containing pyrene. As mentioned earlier, a comparison of the computed binding energies of these structures predict that the Xe_2.py@OA_2 complex is more stable than the Xe.py@OA_2 complex. To probe these possibilities, variable temperature ^{1}H NMR spectra were recorded between 25 and 2 °C (Figure 5v and Figure S11). The signals at 25 °C were broad. As the temperature was lowered, signals sharpened and several of them split into multiple peaks. This is clearly seen in the spectrum displayed in Figure 5v taken at 2 °C. We attribute this to the presence of more than one type of py−Xe−OA complex. Such a possibility is consistent with multiple exponential fluorescence decay of py@OA_2 in the presence of Xe (Figure 3b and Table S2). While the S_1 state of py@OA_2 in aerated buffer solution decays with a single exponential decay with a lifetime of 359 ns (98.9%), in xenon saturated solution, it decayed with several lifetimes of 326 ns (81.5%), 23 ns (14%), and 5.2 ns (4%).

Based on the ^{1}H NMR variation with the gas saturating the solution (Xe or N_2), one would expect an effect on the emission spectrum of encapsulated pyrene. As illustrated in Figure 5b, no phosphorescence was observed from py@OA_2 when the buffer solution was saturated with either air or oxygen; with nitrogen bubbling, a very weak phosphorescence could be recorded, which became stronger with Xe. The strong phosphorescence observed only in the presence of Xe confirms the heavy atom effect facilitated by supramolecular chemistry.

CONCLUSIONS

In this study, we have established that phosphorescence from pyrene at room temperature could be induced by copopulating pyrene confined within a water-soluble organic capsule with a heavy atom like xenon. Although both $TlNO_3$ and xenon are water-soluble, only the latter functions as a heavy atom under our conditions as the former destabilizes the capsular assembly. Computational modeling and NMR studies suggest that xenon remains within the capsule along with the hydrophobic, aromatic pyrene molecule. The observation that xenon is ineffective in prompting phosphorescence when bubbled into a solution of pyrene in water or cyclohexane that accentuates the value of the host OA combined with the elegant supramolecular heavy atom technique in inducing phosphorescence from aromatic molecules at room temperature. Further purging the octa acid with xenon could open up opportunities to examine the properties of clusters of xenon in a confined space.

ASSOCIATED CONTENT

Supporting Information

The Supporting Information is available free of charge on the ACS Publications website at DOI: 10.1021/acs.jpca.9b08354.

^{1}H NMR spectra of host−guest complexes (PDF)

AUTHOR INFORMATION

Corresponding Authors

*E-mail: rpr@miami.edu (R.P.).

*E-mail: murthy1@miami.edu (V.R.).

ORCID

Rajeev Prabhakar: 0000-0003-1137-1272

V. Ramamurthy: 0000-0002-3168-2185

Notes

The authors declare no competing financial interest.

ACKNOWLEDGMENTS

V.R. and R.P. thank the National Science Foundation (CHE-1807729 and CHE-1664926) for financial support. We thank Dr. Perry J. Pellechia of University of South Carolina for Xe NMR spectra.

REFERENCES

(1) McCusker, C. E.; Castellano, F. N. Materials Integrating Photochemical Upconversion. *Top. Curr. Chem.* **2016**, *374*, 1−25.

(2) Singh-Rachford, T. N.; Castellano, F. N. Photon Upconversion Based on Sensitized Triplet−Triplet Annihilation. *Coord. Chem. Rev.* **2010**, *254*, 2560−2573.

(3) Wen, S.; Zhou, J.; Zheng, K.; Bednarkiewicz, A.; Liu, X.; Jin, D. Advances in Highly Doped Upconversion Nanoparticles. *Nat. Commun.* **2018**, *9*, 1−12.

DOI: 10.1021/acs.jpca.9b08354
J. Phys. Chem. A 2019, 123, 9123−9131

(4) Yanai, N.; Kimizuka, N. New Triplet Sensitization Routes for Photon Upconversion: Thermally Activated Delayed Fluorescence Molecules, Inorganic Nanocrystals, and Singlet-to-Triplet Absorption. *Acc. Chem. Res.* **2017**, *50*, 2487−2495.
(5) Ye, C.; Zhou, L.; Wang, X.; Liang, Z. Photon Upconversion: From Two-Photon Absorption (Tpa) to Triplet−Triplet Annihilation (Tta). *Phys. Chem. Chem. Phys.* **2016**, *18*, 10818−10835.
(6) Zhou, J.; Liu, Q.; Feng, W.; Sun, Y.; Li, F. Upconversion Luminescent Materials: Advances and Applications. *Chem. Rev.* **2015**, *115*, 395−465.
(7) Turro, N. J.; Ramamurthy, V.; Scaiano, J. C. *Modern Molecular Photochemistry of Organic Molecules*; University Science Books: Sausalito, CA, 2010.
(8) Easley, C. J.; Mettry, M.; Moses, E. M.; Hooley, R. J.; Bardeen, C. J. Boosting the Heavy Atom Effect by Cavitand Encapsulation: Room Temperature Phosphorescence of Pyrene in the Presence of Oxygen. *J. Phys. Chem. A* **2018**, *122*, 6578−6584.
(9) Wang, X.-F.; Xiao, H.; Chen, P.-Z.; Yang, Q.-Z.; Chen, B.; Tung, C.-H.; Chen, Y.-Z.; Wu, L.-Z. Pure Organic Room Temperature Phosphorescence from Excited Dimers in Self-Assembled Nanoparticles under Visible and Nearinfrared Irradiation in Water. *J. Am. Chem. Soc.* **2019**, *141*, 5045−5050.
(10) Fang, M.; Yang, J.; Xiang, X.; Xie, Y.; Dong, Y.; Peng, Q.; Li, Q.; Li, Z. Unexpected Room-Temperature Phosphorescence from a Non-Aromatic, Low Molecular Weight, Pure Organic Molecule through the Intermolecular Hydrogen Bond. *Mater. Chem. Front.* **2018**, *2*, 2124−2129.
(11) Kenry, C. C.; Liu, B. Enhancing the Performance of Pure Organic room-temperature Phosphorescent Luminophores. *Nat. Commun.* **2019**, *10*, 1−15.
(12) Lv, A.; Ye, W.; Jiang, X.; Gan, N.; Shi, H.; Yao, W.; Ma, H.; An, Z.; Huang, W. Room-Temperature Phosphorescence from Metal-Free Organic Materials in Solution: Origin and Molecular Design. *J. Phys. Chem. Lett.* **2019**, *10*, 1037−1042.
(13) Mu, Y.; Yang, Z.; Chen, J.; Yang, Z.; Li, W.; Tan, X.; Mao, Z.; Yu, T.; Zhao, J.; Zheng, S.; et al. Mechano-Induced Persistent Room-Temperature Phosphorescence from Purely Organic Molecules. *Chem. Sci.* **2018**, *9*, 3782−3787.
(14) Wu, H.; Chi, W.; Chen, Z.; Liu, G.; Gu, L.; Bindra, A. K.; Yang, G.; Liu, X.; Zhao, Y. Achieving Amorphous Ultralong Room Temperature Phosphorescence by Coassembling Planar Small Organic Molecules with Polyvinyl Alcohol. *Adv. Funct. Mater.* **2019**, *29*, 1−10.
(15) Xiao, L.; Fu, H. Enhanced Room-Temperature Phosphorescence through Intermolecular Halogen/Hydrogen Bonding. *Chem. − Eur. J.* **2019**, *25*, 714−723.
(16) Zhou, Y.; Qin, W.; Du, C.; Gao, H.; Zhu, F.; Liang, G. Long-Lived Room-Temperature Phosphorescence for Visual and Quantitative Detection of Oxygen. *Angew. Chem., Int. Ed.* **2019**, *58*, 12102−12106.
(17) Kasha, M. Collisional Perturbation of Spin-Orbital Coupling and the Mechanism of Fluorescence Quenching. A Visual Demonstration of the Perturbation. *J. Chem. Phys.* **1952**, *20*, 71−74.
(18) McGlynn, S. P.; Azumi, T.; Kasha, M. External Heavy-Atom Spin-Orbital Coupling Effect. V. Absorption Studies of Triplet States. *J. Chem. Phys.* **1964**, *40*, 507−515 10.1063/1.1725145. .
(19) McGlynn, S. P.; Daigre, J.; Smith, F. J. External Heavy-Atom Spin-Orbital Coupling Effect. Intersystem Crossing. *J. Chem. Phys.* **1963**, *39*, 675−679.
(20) McGlynn, S. P.; Sunseri, R.; Christodouleas, N. External Heavy-Atom Spin-Orbital Coupling Effect. I. The Nature of the Interaction. *J. Chem. Phys.* **1962**, *3937*, 1818−1824.
(21) Uppili, S.; Marti, V.; Nicolaus, A.; Jockusch, S.; Adam, W.; Engel, P. S.; Turro, N. J.; Ramamurthy, V. Heavy Cation Induced Phosphorescence of Alkanones and Azoalkanes in Zeolites as Hosts: Induced $S_1(n\,\pi^*)$ to $T_1(n\,\pi^*)$ Intersystem Crossing and S_0 to $T_1(n\,\pi^*)$ Absorption. *J. Am. Chem. Soc.* **2000**, *122*, 11025−11026.
(22) Ramamurthy, V.; Caspar, J. V.; Corbin, D. R.; Schlyer, B. D.; Maki, A. H. Triplet-State Photophysics of Naphthalene and α,ω-Diphenylpolyenes Included in Heavy-Cation-Exchanged Zeolites. *J. Phys. Chem.* **1990**, *94*, 3391−3393.
(23) Ramamurthy, V.; Casper, J. V.; Eaton, D. F.; Kuo, E. W.; Corbin, D. R. Heavy Atom Induced Phosphorescence of Aromatics and Olefins Included within Zeolites. *J. Am. Chem. Soc.* **1992**, *114*, 3882−3892.
(24) Ciorba, S.; Clennan, E. L.; Mazzucato, U.; Spalletti, A. Induced Phosphorescence of Some Aza- and Thio-Stilbenes Embedded in Thallium-Exchanged Zeolites. *J. Luminescence* **2011**, *131*, 1193−1197.
(25) Turro, N. J.; Aikawa, M. Phosphorescence and Delayed Fluorescence of 1-Chloronaphthalene in Micellar Solutions. *J. Am. Chem. Soc.* **1980**, *102*, 4866−4870.
(26) Turro, N. J.; Bolt, J. D.; Kuroda, Y.; Tabushi, I. A Study of the Kinetics of Inclusion of Halonaphthalenes with β-Cyclodextrin Via Time Correlated Phosphorescence. *Photochem. Photobiol.* **1982**, *35*, 69−72.
(27) Turro, N. J.; Cox, G. S.; Li, X. Remarkable Inhibition of Oxygen Quenching of Phosphorescence by Complexation with Cyclodextrins. *Photochem. Photobiol.* **1983**, *37*, 149−153.
(28) Turro, N. J.; Liu, K.-C.; Chow, M.-F.; Lee, P. Convinient and Simple Methods for the Observation of Phosphorescence in Fluid Solutions. Internal and External Heavy Atom and Micellar Effects. *Photochem. Photobiol.* **1978**, *27*, 523−529.
(29) Kalyanasundaram, K.; Grieser, F.; Thomas, J. K. Room Temperature Phosphorescence of Aromatic Hydrocarbons in Aqueous Micellar Solutions. *Chem. Phys. Lett.* **1977**, *51*, 501−505.
(30) Hamai, S. Room-Temperature Phosphorescence from 1:1:1 Inclusion Compounds of B-Cyclodextrin with Brominated Alcohols and Acenaphthene. *J. Am. Chem. Soc.* **1989**, *111*, 3954−3957.
(31) Hamai, S. Inclusion Complexes and the Room-Temperature Phosphorescence of 6-Bromo-2-Naphthol in Aerated Aqueous Solution of α-Cyclodextrin. *J. Phys. Chem.* **1995**, *99*, 12109−12114.
(32) Love, L. J. C.; Skrilec, M.; Habarta, J. G. Analysis by Micelle-Stabilized Room Temperature Phosphorescence in Solution. *Anal. Chem.* **1980**, *52*, 754−759.
(33) Scypinski, S.; Love, L. J. C. Room-Temperature Phosphorescence of Polynuclear Aromatic Hydrocarbons in Cyclodextrins. *Anal. Chem.* **1984**, *56*, 322−327.
(34) Petrin, M.; Maki, A. H.; Ghosh, S. Specfic Counterion Effects on Naphthalene Solubilized in Sds Micelles Investigated by Optically Detected Magnetic Resonance. *Chem. Phys. Lett.* **1986**, *128*, 425−431.
(35) Humphry-Baker, R.; Moroi, Y.; Gratzel, M. Perturbation Studies of the Photophysics of Arenes in Functionalized Micellar Assemblies. Drastic Phosphorescence Enhancements. *Chem. Phys. Lett.* **1978**, *58*, 207−210.
(36) Ramamurthy, V. *Photochemistry in Organized & Constrained Media*; VCH: New York, 1991.
(37) Ramamurthy, V.; Inoue, Y. *Supramolecular Photochemistry*; John Wiley & Sons: Hoboken, NJ, 2011.
(38) Segebarth, N.; Aïtjeddig, L.; Locci, E.; Bartik, K.; Luhmer, M. Novel Method for the Measurement of Xenon Gas Solubility Using ^{129}Xe Nmr Spectroscopy. *J. Phys. Chem. A* **2006**, *110*, 10770−10776.
(39) Ramamurthy, V. Organic Guests within Zeolites: Xenon as a Photophysical Probe. *J. Am. Chem. Soc.* **1994**, *116*, 1345−1351.
(40) Horrocks, A. R.; Kearvell, A.; Tickle, K. Wilkinson, Mechanism of Fluorescence Quenching in Solution. Part-2- Quenching by Xenon and Intersystem Crossing Efficiencies. *Trans. Faraday Soc.* **1966**, *62*, 3393−3399.
(41) Horrocks, A. R.; Medinger, T.; Wilkinson, F. Solvent Dependence of the Quantum Yield of Triplet State Productin of 9-Phenylanthracene. *Photochem. Photobiol.* **1967**, *6*, 21−28.
(42) Horrocks, A. R.; Wilkinson, F. Triplet State Formation Efficiencies of Aromatic Hydrocarbons in Solution. *Proc. Roy. Soc. A.* **1968**, *306*, 257−273.
(43) Kearvell, A.; Wilkinson, F. Fluorescence Quenching and External Spin-Orbit Coupling Effects. *Molecular Crystals* **1968**, *4*, 69−81.

DOI: 10.1021/acs.jpca.9b08354
J. Phys. Chem. A 2019, 123, 9123−9131

(44) Calcaterra, L. T.; Schuster, D. I. Observation of an Unprecedented Heavy-Atom Effect on the Rate of ^{1}n,π*->^{3}n,π* in β, γ -Unsaturated Ketone. *J. Am. Chem. Soc.* **1981**, *103*, 2460−2461.
(45) Morrison, H.; Miller, A. An Analysis of Heavy-Atom Perturbation of Intersystem Crossing as a Mechanistic Tool in Photochemistry. *Tetrahedron* **1981**, *37*, 3405−3409.
(46) Carroll, F. A.; Quina, F. H. A New Method for the Determination of Intersystem Crossing Quantum Yields. Application to Benzene and Its Methyl Derivatives. *J. Am. Chem. Soc.* **1976**, *98*, 1−6.
(47) Hutubise, R. J. *Phosphorimetry: Theory, Instrumentation Ans Applications*; VCH Publishers: New York, 1990.
(48) Gibb, C. L. D.; Gibb, B. C. Well-Defined, Organic Nanoenvironments in Water: The Hydrophobic Effect Drives a Capsular Assembly. *J. Am. Chem. Soc.* **2004**, *126*, 11408−11409.
(49) Ramamurthy, V. Photochemistry within a Water-Soluble Organic Capsule. *Acc. Chem. Res.* **2015**, *48*, 2904−2917.
(50) Ramamurthy, V.; Jockusch, S.; Porel, M. Supramolecular Photochemistry in Solution and on Surfaces: Encapsulation and Dynamics of Guest Molecules and Communication between Encapsulated and Free Molecules. *Langmuir* **2015**, *31*, 5554−5570.
(51) Porel, M.; Chuang, C.; Burda, C.; Ramamurthy, V. Ultrafast Photoinduced Electron Transfer between an Incarcerated Donor and a Free Acceptor in Aqueous Solution. *J. Am. Chem. Soc.* **2012**, *134*, 14718−14721.
(52) Chuang, C.-H.; Porel, M.; Choudhury, R.; Burda, C.; Ramamurthy, V. Ultrafast Electron Transfer across a Nanocapsular Wall: Coumarins as Donors, Viologen as Acceptor, and Octa Acid Capsule as the Mediator. *J. Phys. Chem. C* **2017**, *122*, 328−337.
(53) Raj, A. M.; Porel, M.; Mukherjee, P.; Ma, X.; Choudhury, R.; Galoppini, E.; Sen, P.; Ramamurthy, V. Ultrafast Electron Transfer from Upper Excited State of Encapsulated Azulenes to Acceptors across an Organic Molecular Wall. *J. Phys. Chem. C* **2017**, *121*, 20205−20216.
(54) Porel, M.; Jockusch, S.; Parthasarathy, A.; Rao, V. J.; Turro, N. J.; Ramamurthy, V. Photoinduced Electron Transfer between a Donor and an Acceptor Separated by a Capsular Wall. *Chem. Commun.* **2012**, *48*, 2710−2712.
(55) Gupta, S.; Adhikari, A.; Mandal, A. K.; Bhattacharyya, K.; Ramamurthy, V. Ultrafast Singlet-Singlet Energy Transfer between an Acceptor Electrostatically Attached to the Walls of an Organic Capsule and the Enclosed Donor. *J. Phys. Chem. C* **2011**, *115*, 9593−9600.
(56) Porel, M.; Jockusch, S.; Ottaviani, M. F.; Turro, N. J.; Ramamurthy, V. Interaction between Encapsulated Excited Organic Molecules and Free Nitroxides: Communication across a Molecular Wall. *Langmuir* **2011**, *27*, 10548−10555.
(57) Jockusch, S.; Porel, M.; Ramamurthy, V.; Turro, N. J. Cidep from a Polarized Ketone Triplet State Incarcerated within a Nanocapsule to a Nitroxide in the Bulk Aqueous Solution. *J. Phys. Chem. Lett.* **2011**, *2*, 2877−2880.
(58) Jockusch, S.; Zeika, O.; Jayaraj, N.; Ramamurthy, V.; Turro, N. J. Electron Spin Polarization Transfer from a Nitroxide Incarcerated within a Nanocapsule to a Nitroxide in the Bulk Aqueous Solution. *J. Phys. Chem. Lett.* **2010**, *1*, 2628−2632.
(59) Chen, J. Y.-C.; Jayaraj, N.; Jockusch, S.; Ottaviani, M. F.; Ramamurthy, V.; Turro, N. J. An EPR and NMR Study of Supramolecular Effects on Paramagnetic Interaction between a Nitroxide Incarcerated within a Nanocapsule with a Nitroxide in Bulk Aqueous Media. *J. Am. Chem. Soc.* **2008**, *130*, 7206−7207.
(60) Jayaraj, N.; Maddipatla, M. V. S. N.; Prabhakar, R.; Jockusch, S.; Turro, N. J.; Ramamurthy, V. Closed Nanocontainer Enables Thioketones to Phosphoresce at Room Temperature in Aqueous Solution. *J. Phys. Chem. B* **2010**, *114*, 14320−14328.
(61) Steer, R. P.; Ramamurthy, V. Photophysics and Intramolecular Photochemistry of Thiones in Solution. *Acc. Chem. Res.* **1988**, *21*, 380−386.
(62) Birks, J. B. *Photophysics of Aromatic Molecules*; Wiley: New York, 1970.
(63) Jayaraj, N.; Jockusch, S.; Kaanumalle, L. S.; Turro, N. J.; Ramamurthy, V. Dynamics of Capsuleplex Formed between Octaacid and Organic Guest Molecules - Photophysical Techniques Reveal the Opening and Closing of Capsuleplex. *Can. J. Chem.* **2011**, *89*, 203−213.
(64) Porel, M.; Jayaraj, N.; Kaanumalle, L. S.; Maddipatla, M. V. S. N.; Parthasarathy, A.; Ramamurthy, V. Cavitand Octa Acid Forms a Nonpolar Capsuleplex Dependent on the Molecular Size and Hydrophobicity of the Guest. *Langmuir* **2009**, *25*, 3473−3481.
(65) Choudhury, R.; Barman, A.; Prabhakar, R.; Ramamurthy, V. Hydrocarbons Depending on the Chain Length and Head Group Adopt Different Conformations within a Water-Soluble Nanocapsule: ^{1}h Nmr and Molecular Dynamics Studies. *J. Phys. Chem. B* **2012**, *117*, 398−407.
(66) Becke, A. D. Density-Functional Exchange-Energy Approximation with Correct Asymptotic Behavior. *Phys. Rev. A* **1988**, *38*, 3098.
(67) Francl, M. M.; Pietro, W. J.; Hehre, W. J.; Binkley, J. S.; Gordon, M. S.; DeFrees, D. J.; Pople, J. A. Self-Consistent Molecular Orbital Methods. Xxiii. A Polarization-Type Basis Set for Second-Row Elements. *J. Chem. Phys.* **1982**, *77*, 3654−3665.
(68) Frisch, M. J.; Trucks, G. W.; Schlegel, H. B.; Scuseria, G. E.; Robb, M. A.; Cheeseman, J. R.; Scalmani, G.; Barone, V.; Mennucci, B.; Petersson, G. A. et al. *Gaussian 09, Revision D. 01*; Gaussian, Inc.: Wallingford, CT, 2009.
(69) Wang, J.; Wolf, R. M.; Caldwell, J. W.; Kollman, P. A.; Case, D. A. Development and Testing of a General Amber Force Field. *J. Comput. Chem.* **2004**, *25*, 1157−1174.
(70) Goharshadi, E. K.; Abbaspour, M. Molecular Dynamics Simulation of Argon, Krypton, and Xenon Using Two-Body and Three-Body Intermolecular Potentials. *J. Chem. Theory Comput.* **2006**, *2*, 920−926.
(71) Trott, O.; Olson, A. J. Autodock Vina: Improving the Speed and Accuracy of Docking with a New Scoring Function, Efficient Optimization, and Multithreading. *J. Comput. Chem.* **2010**, *31*, 455−461.
(72) Hess, B.; Kutzner, C.; Van Der Spoel, D.; Lindahl, E. Gromacs 4: Algorithms for Highly Efficient, Load-Balanced, and Scalable Molecular Simulation. *J. Chem. Theory Comput.* **2008**, *4*, 435−447.
(73) Price, D. J.; Brooks, C. L., III A Modified Tip3p Water Potential for Simulation with Ewald Summation. *J. Chem. Phys.* **2004**, *121*, 10096−10103.
(74) Darden, T.; York, D.; Pedersen, L. Particle Mesh Ewald: An N·Log(N) Method for Ewald Sums in Large Systems. *J. Chem. Phys.* **1993**, *98*, 10089−10092.
(75) Miyamoto, S.; Kollman, P. A. Settle: An Analytical Version of the Shake and Rattle Algorithm for Rigid Water Models. *J. Comput. Chem.* **1992**, *13*, 952−962.
(76) Hess, B.; Bekker, H.; Berendsen, H. J. C.; Fraaije, J. G. E. M. Lincs: A Linear Constraint Solver for Molecular Simulations. *J. Comput. Chem.* **1997**, *18*, 1463−1472.
(77) Krieger, E.; Vriend, G. Yasara View—Molecular Graphics for All Devices—from Smartphones to Workstations. *Bioinformatics* **2014**, *30*, 2981−2982.
(78) Humphrey, W.; Dalke, A.; Schulten, K. Vmd: Visual Molecular Dynamics. *J. Mol. Graph.* **1996**, *14*, 33−38.
(79) Pettersen, E. F.; Goddard, T. D.; Huang, C. C.; Couch, G. S.; Greenblatt, D. M.; Meng, E. C.; Ferrin, T. E. Ucsf Chimera—a Visualization System for Exploratory Research and Analysis. *J. Comput. Chem.* **2004**, *25*, 1605−1612.
(80) Jayaraj, N.; Zhao, Y.; Parthasarathy, A.; Porel, M.; Liu, R. S. H.; Ramamurthy, V. Nature of Supramolecular Complexes Controlled by the Structure of the Guest Molecules: Formation of Octa Acid Based Capsuleplex and Cavitandplex. *Langmuir* **2009**, *25*, 10575−10586.
(81) Tang, H.; de Oliveira, C. S.; Sonntag, G.; Gibb, C. L. D.; Gibb, B. C.; Bohne, C. Dynamics of a Supramolecular Capsule Assembly with Pyrene. *J. Am. Chem. Soc.* **2012**, *134*, 5544−5547.
(82) Thomas, S. S.; Tang, H.; Gaudes, A.; Baggesen, S. B.; Gibb, C. L. D.; Gibb, B. C.; Bohne, C. Tuning the Binding Dynamics of a

DOI: 10.1021/acs.jpca.9b08354
J. Phys. Chem. A 2019, 123, 9123−9131

Guest-Octaacid Capsule through Non-Covalent Anchoring. *J. Phys. Chem. Lett.* **2017**, *8*, 2573−2578.
(83) Raj, A. M.; Talluri, S. G.; Dubus, M.; Gupta, S.; Mondal, B.; Ramamurthy, V. Probing the pH Dependent Assembly-Disassembly of Water-Soluble Organic Capsules with Coumarins and Anthracene. *J. Photochem. Photobiol., A* **2018**, *355*, 398−407.
(84) Kalyanasundaram, K.; Thomas, J. K. Environmental Effects on Vibronic Band Intensities in Pyrene Monomer Fluorescence and Their Application in Studies of Micellar Systems. *J. Am. Chem. Soc.* **1977**, *99*, 2039−2044.
(85) Dong, D. C.; Winnik, M. A. The Py Scale of Solvent Polarities . Solvent Effects on the Vibronic Fine Structure of Pyrene Fluorescence and Empirical Correlations with $E_T$and Y Values. *Photochem. Photobiol.* **1982**, *35*, 17−21.
(86) Dong, D. C.; Winnik, M. A. The Py Scale of Solvent Polarities. *Can. J. Chem.* **1984**, *62*, 2560−2565.
(87) Fogarty, H. A.; Berthault, P.; Brotin, T.; Huber, G.; Desvaux, H.; Dutasta, J.-P. A Cryptophane Core Optimized for Xenon Encapsulation. *J. Am. Chem. Soc.* **2007**, *129*, 10332−10333.
(88) Bartik, K.; Luhmer, M.; Dutasta, J.-P.; Collet, A.; Reisse, J. ^{129}Xe and ^{1}H Nmr Study of the Reversible Trapping of Xenon by Cryptophane-a in Organic Solution. *J. Am. Chem. Soc.* **1998**, *120*, 784−791.
(89) Huber, G.; Brotin, T.; Dubois, L.; Desvaux, H.; Dutasta, J.-P.; Berthault, P. Water Soluble Cryptophanes Showing Unprecedented Affinity for Xenon: Candidates as NMR-Based Biosensors. *J. Am. Chem. Soc.* **2006**, *128*, 6239−6246.
(90) Branda, N.; Grotzfeld, R. M.; Valdes, C.; Rebek, J. J. Control of Self-Assembly and Reversible Encapsulation of Xenon in a Self-Assembling Dimer by Acid—Base Chemistry. *J. Am. Chem. Soc.* **1995**, *117*, 85−88.
(91) Robbins, T. A.; Knobler, C. B.; Bellew, D. R.; Cram, D. J. Host-guest complexation. 67. A Highly Adaptive and Strongly Binding Hemicarcerand. *J. Am. Chem. Soc.* **1994**, *116*, 111−122.
(92) Cao, Q.; Andrijchenko, N.; Ermilov, A.; Räsänen, M.; Nemukhin, A.; Khriachtchev, L. Interaction of Aromatic Compounds with Xenon: Spectroscopic and Computational Characterization for the Cases of P-Cresol and Toluene. *J. Phys. Chem. A* **2015**, *119*, 2587−2593.

DOI: 10.1021/acs.jpca.9b08354
J. Phys. Chem. A 2019, 123, 9123−9131